

# Supporting Information

Kawasaki and Tanaka 10.1073/pnas.1001040107

## SI Text

**Comparison of Slow Glassy Dynamics of Supercooled Colloidal Suspensions Between Brownian Dynamics (BD) Simulations and Confocal Microscopy Experiments.** To show how powerful BD simulations are, we compare results of slow glassy dynamics of supercooled colloidal suspensions between BD simulations with the canonical, constant temperature–constant volume (NVT) ensemble and confocal microscopy experiments. In confocal experiments, we can track the coordinates of individual particles as a function of time in 3D. In both BD simulations and confocal microscopy experiments, thus, we can calculate the structural relaxation time  $\tau_\alpha$  from the decay of the self part of the intermediate scattering function  $F_s(q_p, t)$ , where  $q_p$  is the wavenumber corresponding to the first peak of the structure factor  $S(q)$ . Fig. S1 shows a comparison of  $\tau_\alpha$  obtained in this way between BD simulations and confocal experiments. The results of our BD simulations almost perfectly coincide with those of our confocal microscopy experiments of colloidal suspensions (by Mathieu Leocmach in our group) without any adjustable parameters, indicating the potential of brute-force BD simulations for crystal nucleation phenomena.

**Finite Size Effects on the Crystal Nucleation Frequency.** Here we study the finite size effects on crystal nucleation. In our NVT simulations, crystal nucleation necessarily leads to the formation of depleted regions around nuclei, reflecting the conservation of the particle density (see Fig. 5). This nonlocal coupling might lead to significant finite size effects. We have checked this result by changing the system size. As shown in Fig. S2, there are almost no finite size effects for a system containing more than 4,000 particles. Although there appears finite size effects for  $N = 1,024$ , even for this case the effects on the crystal nucleation frequency  $I_r$  are rather weak (less than a factor of 10) (see Fig. S2D). So the finite size effects cannot explain the large discrepancy in  $I_r$  between us and Auer and Frenkel (1). We recently confirmed (2) that there are few finite size effects on MRCO also for  $N \geq 4,096$  in an accessible  $\phi$  range. This result is consistent with the above results, on noting that a crystal nucleus always appears inside a region of high MRCO and thus the critical nucleus size should be smaller than the characteristic size of MRCO.

**Crystal Nucleation Process in a System of  $N=4,096$ .** Here we show a crystal nucleation process in a system of a smaller size ( $N = 4,096$ ) in Fig. S3, because it may be easier to see the details of crystal nucleation for a smaller system (see also [Movie S2](#)).

**Comparison Between the Coarse-Grained Sixfold Bond Orientational Order Parameter  $Q_6$  and  $S_{ij}$ .** First we review the discussion by Lechner and Dellago (3) on how the choice of an order parameter affects the detection of crystalline order. First we mention that  $S_{ij}$ , which measures the correlation between the structures surrounding particles  $i$  and  $j$ , distinguishes between solid- and liquid-like particles but does not discriminate between different crystal structures. This insensitivity of  $S_{ij}$  to the difference in crystal structures is actually the very reason why this parameter is used by Auer and Frenkel in their study of the kinetics of crystal nucleation (1) (see below). Lechner and Dellago (3) showed that the crystal structure determination can be improved by using the spatially averaged form of the local bond order parameters  $Q_6^i$  (see *Materials and Methods*), which we used in our study. To calculate  $Q_6^i$ , one uses the local orientational order vectors  $\vec{q}_{6m}^i$  averaged over particle  $i$  and its surroundings. Although  $q_6^i$  (see

*Materials and Methods* for the definition) holds the information of the structure of the first shell around particle  $i$ , its spatially averaged version  $Q_6^i$  also takes into account the second shell. They concluded that using the parameter  $Q_6^i$  instead of  $q_6^i$  increases the accuracy of the distinction of different crystal structures at the price of a coarsening of the spatial resolution. We find that medium-range crystalline order (MRCO) in a supercooled liquid can be detected by both  $Q_6^i$  and  $S_{ij}$  (see below) but not so well by  $q_6^i$ . This difference arises from the fact that the second particle shell is effectively taken into account in both  $Q_6^i$  and  $S_{ij}$ , but not in  $q_6^i$  (3). Thus,  $q_6^i$  is not a good measure to detect the bond orientational order (MRCO) in a supercooled liquid. Note that  $q_6^i$  is not so resistive to fluctuations, which are large in a liquid state. Some coarse-graining of the order parameter seems to be essential to detect hidden structural order in a supercooled liquid.

In Fig. S4A, we show the distribution of  $S_{ij} = \mathbf{q}_6(i) \cdot \mathbf{q}_6(j)$  (here \* means the complex conjugate) for an equilibrium and a supercooled liquid and body-centered cubic (bcc), hcp, random hexagonal close packing (rhcp), and face-centered cubic (fcc) crystals. This parameter was used by Auer and Frenkel (1) as the order parameter to characterize crystal nuclei and its kinetic pathway of crystallization. If we set the threshold at  $S_{ij} = 1.5$ , we can distinguish a supercooled liquid and crystals. However, this criterion cannot allow us to detect MRCO in a supercooled liquid, as can be seen in Fig. S4B: There are very few yellow particles there. On the other hand, we can distinguish high MRCO regions by using  $Q_6$  as shown in Fig. S4C. A similar pattern can be detected even by  $S_{ij}$  if we set the threshold at  $S_{ij} \geq 0.75$  (see blue particles in Fig. S4B and compare it with C). Then, however, we cannot distinguish crystal nuclei from high MRCO regions with this single threshold. On the other hand, we can see crystals clearly if we set  $S_{ij} = 1.5$  or  $Q_6 = 0.4$ , as shown in Fig. S4D and E. This result means that we need at least two thresholds for the order parameter,  $S_{ij}$  or  $Q_6$ , to detect both MRCO and crystals separately. Furthermore, to detect the continuous development of MRCO in a supercooled liquid with an increase in  $\phi$ , we need to see the change of the distribution (or at least the average value) of  $Q_6$  or  $S_{ij}$ . As discussed in the main text, structural ordering in a supercooled liquid should decrease its free energy, which affects the free-energy gain upon crystal formation as well as the interfacial energy cost for creating crystal nuclei. So it may be crucial to characterize the structural order in a supercooled liquid before and after nucleation.

**Possible origins of the discrepancy between our results and those of Auer and Frenkel (1) on crystal nucleation frequency.** Here we discuss possible causes of the difference between our results and those of Auer and Frenkel (1). To do so, we first explain their approach. They used the fact that the crystallization rate is the product of a static term, i.e., the probability for the formation of a critical nucleus  $P_c$ , and a kinetic factor  $\Gamma$  that describes the rate at which such nuclei grow. Then they used umbrella sampling (with a biased potential) to compute the former ( $P_c$ ) and kinetic Monte Carlo simulations to compute the latter ( $\Gamma$ ). The combined nucleation rate was compared to experimental data. This method is elegant, but requires a few assumptions. For example, to estimate  $P_c$ , we need to define a reaction coordinate that measures the degree of crystallinity of the system. So we need a structural order parameter sensitive to the crystallinity itself, but insensitive to the difference between possible crystal structures. This latter requirement is so to use the biased sampling, which enhances the probability having crystal clusters around a certain size but



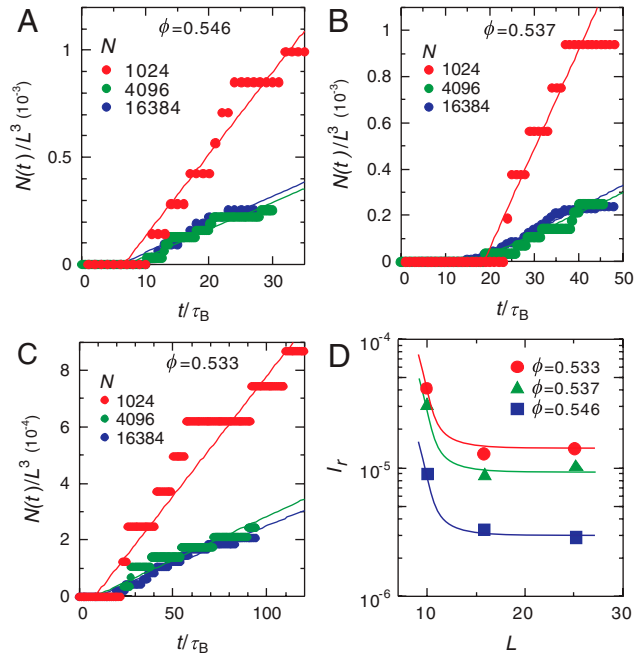


**Fig. S2.** System size dependence of the crystal nucleation. Temporal change of the number of crystal nuclei for three systems ( $N = 1,024$ ;  $4,096$ ; and  $16,834$ ) for  $\phi = 0.546$  (A),  $\phi = 0.537$  (B), and  $\phi = 0.533$  (C). (D) System size dependence of the reduced crystal nucleation frequency  $I_r$ , which is estimated from the rate of the increase in the number of crystal nuclei (A–C). We can see that there is almost no system size dependence for  $N \geq 4,096$ .

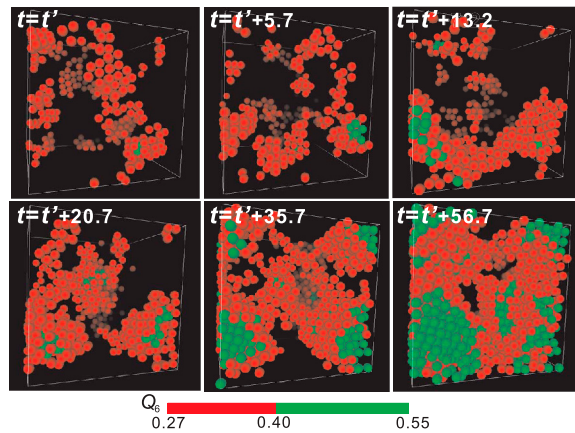
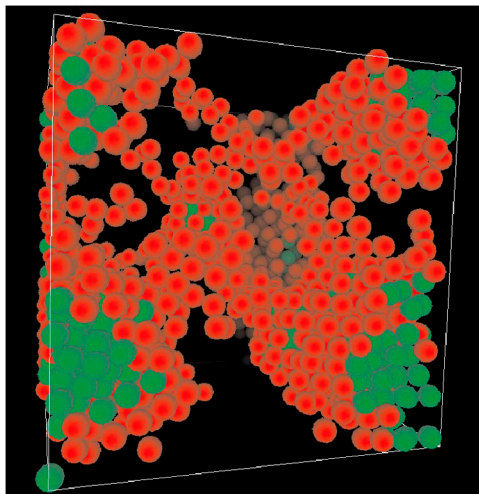


**Fig. S3.** Birth of a crystal nucleus from medium-range structural order. The process of nucleation of a crystal at  $\phi = 0.537$  ( $N = 4,096$ ) (see also [Movie S2](#)). Particles with intermediate  $Q_6$  ( $0.27 \leq Q_6 \leq 0.40$ ) are colored red, whereas those with high  $Q_6$  ( $Q_6 \geq 0.4$ ) are colored green. The time unit is the Brownian time of a particle,  $\tau_B$ . We can see the birth of a crystal and its growth. Time  $t = t'$  is when a supercooled liquid reaches a sort of quasi-equilibrium steady state after the initiation of simulations from a random disordered state.





**Movie S2.** A birth process of a crystal nucleus from medium-range structural order in a supercooled liquid ( $N = 4,096$ ) at  $\phi = 0.537$  (the same process as in Fig. S3). Because of the small size of the system, we can see more details of a nucleation process of crystals. Particles with higher  $Q_6$  ( $Q_6 \geq 0.27$ ) are colored red, whereas those with even higher  $Q_6$  ( $Q_6 \geq 0.4$ ) are colored green. The entire process corresponds to about  $60 \tau_B$  ( $\tau_B$ , the Brownian time of a particle).

[Movie S2 \(AVI\)](#)